

1  
2  
3  
4  
5  
6  
7  
8  
9  
10  
11  
12  
13  
14  
15  
16  
17  
18  
19  
20  
21  
22  
23  
24  
25  
26  
27

**Inhibition of Notch signaling reduces the number of surviving Dclk1+ reserve crypt epithelial stem cells following radiation injury**

Dongfeng Qu<sup>1,2</sup>, Randal May<sup>1,2</sup>, Sripathi Sureban<sup>1,2,3</sup>, Nathaniel Weygant<sup>1</sup>, Parthasarathy Chandrakesan<sup>1</sup>, Naushad Ali<sup>1</sup>, Linheng Li<sup>4</sup>, Terrence Barrett<sup>5</sup>, Courtney W. Houchen<sup>1,2,3</sup>

<sup>1</sup>Department of Medicine, University of Oklahoma Health Science Center, Oklahoma City, OK 73104

<sup>2</sup>Department of Veterans Affairs Medical Center, Oklahoma City, OK 73104

<sup>3</sup>Peggy and Charles Stephenson Oklahoma Cancer Center, Oklahoma City, OK 73104

<sup>4</sup>Stowers Institute for Medical Research, Kansas City, MO 64110

<sup>5</sup>Department of Medicine, Northwestern University Feinberg School of Medicine, Chicago, IL 60611

**Address correspondence to:** Courtney W. Houchen, M.D  
Department of Medicine, Digestive Disease and Nutrition,  
The University of Oklahoma Health Science Center,  
Oklahoma City, OK 73104  
Phone (405) 271-2175; Fax: (405) 271-5450  
E-mail: Courtney-houchen@ouhsc.edu

**Running title:** Dclk1 and Notch signaling in ISC survival

**Author Contributions:** D.Q., R.M., S.S., and C.W.H. designed research; D.Q., R.M., S.S., N.W., and P.C. performed research; L.L and T.B contributed new reagents; D.Q., R.M., S.S., N.A., and C.W.H. analyzed data; and D.Q. and C.W.H. wrote the manuscript.

28 **Abstract**

29 We have previously reported that doublecortin-like kinase 1 (Dclk1) is a putative intestinal  
30 stem cell (ISC) marker. In this report, we evaluated the use of Dclk1 as a marker of  
31 surviving ISCs in response to treatment with high-dose total body irradiation (TBI). Both  
32 apoptotic and mitotic Dclk1+ cells were observed 24 h post TBI associated with a  
33 corresponding loss of intestinal crypts observed at 84 h post TBI. Although the Notch  
34 signaling pathway plays an important role in regulating proliferation and lineage  
35 commitment within the intestine, its role in ISC function in response to severe genotoxic  
36 injury is not yet fully understood. We employed the microcolony assay to functionally  
37 assess the effects of Notch inhibition with DAPT on intestinal crypt stem cell survival  
38 following severe (> 8 Gy) radiation injury. Following treatment with DAPT, we observed a  
39 nearly 50% reduction in the number of surviving Dclk1+ crypt epithelial cells at 24 h after  
40 TBI and similar reduction in the number of surviving small intestinal crypts at 84 h. These  
41 data indicate that inhibition of Notch signaling decreases ISC survival following radiation  
42 injury, suggesting that the Notch signaling pathway plays an important role in ISC mediated  
43 crypt regeneration. These results also suggest that crypt epithelial cell Dclk1 expression  
44 can be used as one potential marker to evaluate the early survival of ISCs following severe  
45 radiation injury.

46

47 **Keywords:** DCLK1, Notch, stem cells, radiation, crypt survival

48

49

50

51 **Introduction**

52           The adult intestinal epithelium is continuously and rapidly replaced by cell replication  
53 within the crypts of Lieberkuhn and subsequent migration of their progeny onto the villus  
54 epithelium in the small intestine, or onto the surface epithelium in the colon (9). Intestinal  
55 epithelial cells are ultimately derived from multipotent stem cell(s) located near the base of  
56 each intestinal crypt (3, 4, 32, 37). In the adult mouse small intestine, these crypt stem cells  
57 divide to produce a daughter stem cell (self-renewal) as well as a more rapidly replicating  
58 transit cell. Their progeny subsequently differentiate into the mature epithelial cell types  
59 found in the small intestine as the epithelial cells migrate away from the proliferative zone in  
60 each intestinal crypt (3, 26, 27).

61           Crypt stem cells also play a central role in mucosal regeneration following injury  
62 (22). Intestinal injury induced by genotoxic/cytotoxic agents can disrupt the epithelial barrier  
63 resulting in the loss of crypts. Restoration of normal epithelial architecture and barrier  
64 function is a multistep process: (a) stem cells proliferate to increase their numbers and to  
65 give rise to the more rapidly proliferating transit cell population; (b) the transit cell  
66 population expands rapidly to form a regenerative crypt; and (c) normal patterns of  
67 epithelial differentiation are reestablished by migration and differentiation of cells produced  
68 in these regenerative crypts (9). Moreover, if the injury has completely destroyed some  
69 crypts, the surviving crypt stem cells can divide to replete the number of viable crypts (22).

70           A functional assay for quantifying stem cell survival following acute radiation injury to  
71 the replicating cell population has been developed based on the capacity of the surviving  
72 stem cells to regenerate crypt-like foci of cells (termed microcolonies) (22, 38). The actively  
73 proliferating transit cells are the most sensitive to ionizing radiation-induced injury; the

74 slowly proliferating stem cells are less sensitive to radiation. In this assay, 3 or 4 d after  
75 irradiation, the number of crypt-like foci of surviving epithelial cells is scored on histologic  
76 sections of intestine. Each epithelial foci is thought to represent the survival of one or more  
77 clonogenic stem cells able to give rise to the regenerative crypt. This assay allows for  
78 quantitative assessment of the role of exogenous agents and or molecular signal  
79 transduction pathways on crypt survival and indirectly stem cell survival following lethal  
80 dose total body irradiation.

81 We have reported that doublecortin-like kinase 1 (Dclk1), previously know as  
82 DCAMKL-1, is a putative ISC marker (14, 15). Dclk1+ cells were primarily found at the +4  
83 position of the normal uninjured mouse intestinal crypt. Dclk1+ cells were also found in  
84 other positions along the crypt villus axis including crypt based columnar cells (15). Some  
85 Dclk1+ cells, particularly on the villus, appear to be cells with the morphologic appearance  
86 of Tuft/brush cells (8). The precise function of this morphologically distinct cell remains  
87 unknown. Yet in the crypt, Dclk1 also appears to mark a subpopulation of non-Tuft cells  
88 and occasionally Lgr5 expressing cells (15). In a modified label retention (following 10 Gy  
89 IR) assay, Dclk1 label-retaining cells were functionally quiescent and appeared to be  
90 functionally “anchored” at or near the +4 position (15). These data suggest that post  
91 radiation injury, all of the label retaining Dclk1+ cells are not sloughed off at the villus tip.  
92 Furthermore, Dclk1+ cells sorted from the mouse small intestine using anti-Dclk1 antibody  
93 form spheroids in suspension culture and develop into nodules when injected into the  
94 flanks of athymic nude mice. These nodules contain cells demonstrating markers of early  
95 intestinal epithelial lineage commitment (15). These studies demonstrate that Dclk1 cells  
96 isolated from intestinal crypts have self-renewal capacity.

97           The Notch signaling pathway plays an important role in the regulation of critical  
98 biological processes, including cellular proliferation and lineage commitment within the  
99 intestine. Inhibition of Notch signaling accelerates epithelial differentiation, while over-  
100 activation results in inhibition of all secretory lineage commitment and amplification of the  
101 intestinal progenitor pool (6). The Notch signaling pathway is considered as an intestinal  
102 stem and progenitor cell gatekeeper (13). Whether the Notch signaling pathway plays a  
103 role in ISC functions in response to radiation is not clear.

104           In this report we investigated the effects of inhibiting the Notch signaling pathway  
105 using DAPT on the number of surviving crypts 3.5 days after IR. We also evaluated the  
106 effects of Notch inhibition on the number of Dclk1+ crypt epithelial cells at 24 h after IR. Our  
107 results demonstrate that the effect of Notch inhibitor on Dclk1+ crypt epithelial cells was  
108 proportional to the effect on surviving crypts, which suggests that Dclk1+ cells may provide  
109 a useful surrogate for evaluating the survival of ISCs following radiation injury. This study  
110 also demonstrates that inhibition of Notch signaling decreases ISC survival with an  
111 associated loss of surviving Dclk1+ stem cells following radiation injury, suggesting that the  
112 Notch signaling pathway plays an important role in ISC mediated crypt regeneration.

113

114

115

116

117

118

119

120

121 **Materials and Methods**

122 *Experimental animals.* Six to eight-wk-old female C57Bl/6 mice (The Jackson laboratory,  
123 Bar Harbor, ME) were used in the experiments. Mice were housed under controlled  
124 conditions, including a 12-h light-dark cycle, with ad libitum access to food and water. All  
125 animal experiments were performed with the approval and authorization from the  
126 Institutional Review Board and the Institutional Animal Care and Use Committee, University  
127 of Oklahoma Health Sciences Center.

128 *Irradiation procedure.* Adult mice were exposed to TBI with air being pumped into the  
129 chamber during exposure. A Gamma-cell 40 <sup>137</sup>Cs gamma irradiator was used with a dose  
130 rate of 1 Gy IR per minute. For Difluorophenacetyl-L-alanyl-S-phenylglycine t-butyl ester  
131 (DAPT, Sigma Aldrich, St. Louis, MO) treatment, mice (n=5) were injected with DAPT (100  
132 mg/kg in corn oil, *i.p.*) 24 h prior to IR exposure. Mice in the control group (TBI without  
133 DAPT, n=5) were injected with corn oil only. Two hours before the 84 h time interval, each  
134 mouse was injected with 5-bromo-2'-deoxyuridine (BrdU, Sigma Aldrich, St. Louis, MO, 200  
135 µl of 5 mg/ml BrdU solution in PBS). Mice were euthanized at 6, 24, or 84 h post IR  
136 exposure.

137 *Immunohistochemistry.* Heat-induced epitope retrieval was performed on 4-µm formalin-  
138 fixed paraffin-embedded sections by utilizing a pressurized Decloaking Chamber (Biocare  
139 Medical, Concord, CA) in citrate buffer (pH 6.0) at 99°C for 18 min. For brightfield  
140 microscopy, slides exposed to peroxidase blocking solution prior to the addition of primary  
141 antibodies (anti-Dclk1 ab31704, 1:8000 dilution [Abcam, Cambridge, MA], anti-p-β-cat-  
142 Ser552, 1:500 dilution, anti-Ki67, 1:1000). After incubation with primary antibody overnight  
143 at 4°C, the slides were incubated in peroxidase-conjugated polymer (Promark Series-

144 Biocare Medical, CA). Slides were developed with either Betazoid DAB or Bajoran Purple  
145 HRP chromogens (Biocare Medical). To detect apoptotic cells, ApopTag Peroxidase in Situ  
146 Apoptosis Detection Kit was used following the manufacturer's instructions (Millipore,  
147 Billerica, MA). The apoptotic cells were detected with anti-digoxigenin conjugated with  
148 FITC. To detect Dclk1+ apoptotic cells, following the incubation with anti-Dclk1 polyclonal  
149 antibody, anti-rabbit secondary antibody conjugated with Alexa 547 was used.

150 *Microscopic examination.* Slides were examined with a Nikon 80i microscope and  
151 DXM1200C camera for brightfield microscopy. Fluorescent images were taken with  
152 PlanFluoro objectives, utilizing a CoolSnap ES2 camera (Photometrics, Tucson, AZ).  
153 Images were processed using NIS-Elements software (Nikon Instruments, Melville, NY).

154 *Crypt survival study.* The number of surviving crypts was scored across each intestinal  
155 cross-section circumference (a surviving crypt was defined as containing five or more  
156 adjacent, BrdU-positive nuclei (7)). Twenty cross sections were measured for each mouse  
157 and four mice per experimental group.

158 *Real-time RT-PCR Analyses.* Total RNA isolated from small intestine was subjected to  
159 reverse transcription using Superscript™ II RNase H-Reverse Transcriptase and random  
160 hexanucleotide primers (Invitrogen, Carlsbad, CA). The complementary DNA (cDNA) was  
161 subsequently used to perform real-time polymerase chain reaction (PCR) by SYBR™  
162 chemistry (SYBR Green I, Molecular Probes, Eugene, OR) for specific transcripts using  
163 gene-specific primers and JumpStart™ Taq DNA polymerase (Sigma-Aldrich, St. Louis,  
164 MO). The crossing threshold value assessed by real-time PCR was noted for the  
165 transcripts and normalized with  $\beta$ -actin messenger RNA (mRNA). The quantitative changes  
166 in mRNA were expressed as fold-change relative to control  $\pm$  SEM value.

167 The following primers were used:

168  $\beta$ -actin: forward: 5'-GGTGATCCACATCTGCTGGAA-3',

169 reverse: 5'-ATCATTGCTCCTCCTCAGGG-3';

170 Dclk1: forward: 5'- CAGCAACCAGGAATGTATTGGA -3',

171 reverse: 5'- CTCAACTCGGAATCGGAAGACT-3';

172  
173 Notch1: forward: 5'-CGGGTCCACCAGTTTGAATG-3',

174 reverse: 5'-GTTGTATTGGTTCGGCACCAT-3'.

175 Hes1: forward: 5'-TCTGACCACAGAAAGTCATCA -3',

176 reverse: 5'-AGCTATCTTTCTTAAGTGCATC -3';

177

178 *Statistical analysis.* All experiments were performed in triplicate. Results were reported as  
179 average $\pm$  SEM. Data was analyzed using the Student's t test for comparison of mean  
180 values between groups. A *P value* <0.05 was considered statistically significant.

181

182

183

184

185

186

187

188

189

190



191 **Results**

192 ***Intestinal crypt response to total body irradiation.***

193 Adult C57Bl/6 mice were subjected to 12 Gy TBI to study the response of the small  
194 intestinal crypt to genotoxic injury. The small intestines were isolated at 6, 24, 84 and 168 h  
195 post TBI, fixed and stained with H&E (Figure 1). Morphologically apoptotic cells appeared  
196 at 6 h post radiation, suggesting the initiation of cell death induced by radiation damage.  
197 Morphologically mitotic cells appeared at 24 h post radiation, suggesting the release of  
198 stem/progenitor cells from radiation-induced cell cycle arrest allowing surviving  
199 stem/progenitor cells to divide following radiation injury. Regenerative crypts appeared at  
200 3.5 days post radiation, and the return of normal crypt/villus axis architecture appeared at 7  
201 days post radiation even though the crypt was still hyperplastic.

202

203 ***Response of Dclk1+ crypt cells and small intestinal crypts to total body irradiation.***

204 To investigate the response of Dclk1+ crypt epithelial cells and intestinal crypts to genotoxic  
205 injury, C57Bl/6 mice were subjected to 12 Gy TBI. Apoptotic cells were identified by TUNEL  
206 assay at both 6 h and 24 h post TBI (Figure 2, center panel, green staining). Dclk1 in the  
207 crypt cells was identified by specific antibody immunostaining (Figure 2, left panel, red  
208 staining). Dclk1 staining was observed occasionally in apoptotic cells at both 6 h and 24 h  
209 post TBI (Figure 2, right panel for overlay), indicating apoptosis of potential resident stem  
210 cells after high dose radiation injury. Approximately 15% of Dclk1 positive cells were  
211 detected undergoing apoptosis at both 6 h and 24 h post TBI. In our previous report,  
212 apoptotic Dclk1 positive cells were only found at 24 h after low dose radiation (6 Gy), but  
213 not found at 6 h post 6 Gy radiation (14). These data suggested that Dclk1 cells were

214 resistant to low dose IR at 6 h. Moreover, these studies suggested that the 24 h mitotic  
215 activity of Dclk1+ cells could compensate for any stem cell loss as there is essentially no  
216 substantial crypt loss at doses below 8 Gy. He et al. have reported that ISCs that undergo  
217 crypt fission and crypt budding contain nuclear phosphorylated  $\beta$ -catenin-Ser552 (p- $\beta$ -cat-  
218 Ser552) (10). In order to assess this following TBI, crypt cells were immunostained with  
219 anti-p- $\beta$ -cat-Ser552 antibody 24 h post TBI. We found nuclear p- $\beta$ -cat-Ser552 staining in  
220 the crypts, indicating the presence of mitotic stem cells (Figure 3, black arrows in all three  
221 sections). Dclk1 in the crypt cells was identified by specific antibody immunostaining  
222 (Figure 3, purple arrows in all three sections). Moreover, Dclk1 positive cells were found  
223 adjacent to or co-localized with p- $\beta$ -cat-Ser552 positive cells with approximately 40%  
224 incidence (Figure 3, black arrowheads). Furthermore, Dclk1 staining was also found in  
225 some Ki67 positive cells 24 h post 12 Gy IR (Figure 4). These data suggest that the  
226 potential descendants of Dclk1+ cells are able to divide and proliferate 24 h after high dose  
227 TBI. We also observed the loss of intestinal crypts 84 h post 12 Gy again demonstrating the  
228 high dose requirement for crypt loss following TBI (Figure 6A). These results provide  
229 additional support for the long-standing Potten hypothesis that lethal dose (12 Gy) IR  
230 induces crypt stem cell sterilization in a majority of intestinal crypts and the descendants of  
231 the few surviving cells are able to divide and ultimately repopulate the entire intestinal  
232 epithelium (25, 28, 30).

233

234 ***Inhibition of the Notch signaling pathway reduces surviving Dclk1+ cells in response***  
235 ***to TBI.***

236 In uninjured adult mice, there are approximately 20-30 Dclk1+ cells per cross section (~150  
237 crypts) (Data not shown). 24 h post TBI, there are approximately 11 Dclk1+ cells per cross  
238 section counted (Figure 5A), a greater than 50% reduction. This reduction is presumably  
239 the result of apoptotic cell death induced by radiation injury. Apoptotic Dclk1+ cells were  
240 detected post TBI (Figure 2). To investigate the role of the Notch signaling pathway on  
241 crypt epithelial Dclk1+ cell fate after TBI, mice were treated with the  $\gamma$ -secretase inhibitor,  
242 DAPT, 24 h prior to IR exposure. DAPT treatment alone for 48 h didn't affect the number of  
243 Dclk1+ cells per cross section (data not shown). Following DAPT pre-treatment and 24 h  
244 post IR exposure, there were approximately 6 Dclk1+ cells per cross section (Figure 5B,  
245 5C), an approximately 50% reduction in the number of Dclk1+ crypt epithelial cells after  
246 DAPT treatment. These data suggest that Notch signaling pathway plays an important role  
247 in the survival of Dclk1 expressing cells measured *in situ* 24 h after TBI, and inhibition of  
248 Notch pathway may sensitize Dclk1 cells to the effects of high dose TBI.

249

250 ***Inhibition of Notch signaling pathway reduces the number of regenerative crypts in***  
251 ***response to TBI.***

252 Lethal TBI injury induces crypt stem cell sterilization in a majority of intestinal crypts (11).  
253 The appearance of regenerative crypts 84 h post radiation injury is thought to represent the  
254 survival of at least one progenitor/stem cell per crypt (22). There were several BrdU  
255 incorporated crypts (regenerative crypts) detected 84 h post TBI (Figure 6A, brown stain).  
256 After DAPT pre-treatment and 12 Gy IR exposure, the number of BrdU incorporated crypts  
257 were dramatically decreased (Figure 6B). The number of BrdU+ cells per cross section  
258 were quantified and an approximately 50% reduction in crypt survival was observed (Figure

259 6C). These data taken together suggest that the Notch signaling pathway plays an  
260 important role in crypt stem cell survival and/or crypt regeneration following severe  
261 radiation injury.

262

263 ***Inhibition of Notch signaling pathway reduces Dclk1 expression levels in the small***  
264 ***intestine in response to high-dose radiation injury.***

265 In our previous report, immunoreactive Dclk1 staining was not observed in regenerative  
266 crypt epithelial cells 84 h post TBI (14). Restoration of Dclk1 expression within the crypts  
267 was only observed 7 days post radiation injury when the morphologic features of the  
268 intestine are returning to normal. In this study, we measured Dclk1 mRNA levels by  
269 quantitative real time RT-PCR, 24 and 84 h post-IR with or without DAPT pre-treatment. In  
270 the DAPT alone groups, Dclk1 mRNA levels were decreased in intestine approximately  
271 20% and 30% 48 h and 108 h post DAPT pre-treatment, respectively (Figure 7A, dotted  
272 bars of 24 h and 84 h. Note: 24 h and 84 h in this figure indicate for post TBI time, DAPT  
273 pre-treatment started 24 h prior to TBI). This result suggests that the Notch signaling  
274 pathway regulates Dclk1 expression in the small intestine. In the 24 h post TBI groups,  
275 Dclk1 mRNA levels decreased by 60% in the absence of DAPT, and approximately 50% in  
276 the presence of DAPT (Figure 7A). Thus there was no further reduction of Dclk1 mRNA  
277 levels in the presence of DAPT. In the 84 h post TBI groups, Dclk1 mRNA levels decreased  
278 about 45% in the absence of DAPT, and approximately 70% in the presence of DAPT.  
279 Since regenerative crypts at 84 h post IR were reduced 50% in the presence of DAPT  
280 (Figure 6), these data taken together support the hypothesis that inhibition of Notch  
281 signaling results in a reduction in the number of Dclk1 expressing cells.

282

283 We also measured mRNA levels of Notch1, and Hes1, one of the down-stream effectors of  
284 Notch signaling pathway, in the small intestine after DAPT and TBI treatment. In the DAPT  
285 alone groups, Notch1 mRNA levels decreased approximately 40% 24 h after treatment,  
286 and more than 50% 48 and 108 h after treatment (Figure 7B, dotted bars of 0 h, 24 h, and  
287 84 h groups. Note: 24 h and 84 h indicate for post TBI time, DAPT pre-treatment started 24  
288 h prior to TBI). In the 24 h post TBI groups, Notch1 mRNA levels decreased dramatically in  
289 the absence of DAPT, and DAPT treatment furthered the reduction (Figure 7B). In the 84 h  
290 post TBI groups, Notch1 mRNA levels recovered more than 30% in the absence of DAPT,  
291 but remained decreased (70%) in the presence of DAPT. In the DAPT alone groups, Hes1  
292 mRNA levels remained unchanged 24 h after DAPT treatment, but decreased significantly  
293 (30%) after 48 h, and recovered back to baseline levels 108 h after DAPT (Figure 7C,  
294 dotted bars). In the 24 h post TBI groups, Hes1 mRNA levels decreased 60% in the  
295 absence of DAPT, and 50% in the presence of DAPT (Figure 7C). In the 84 h post TBI  
296 groups, Hes1 mRNA levels increased about 30% in the absence of DAPT, and remained  
297 decreased (60% reduction) in the presence of DAPT. These results suggest that the Notch  
298 signaling pathway is very active during crypt regeneration, supporting its importance in  
299 crypt stem epithelial cell dynamics after radiation injury.

300

301

302

303

304

305 **Discussion**

306 In this study we detected apoptotic and mitotic Dclk1+ cells at 24 h, and loss of  
307 crypts at 84 h post 12 Gy TBI. Using Notch pathway inhibitor DAPT, we demonstrated the  
308 effect of Notch inhibitor on Dclk1+ crypt epithelial cells was proportional to the effect on  
309 surviving crypts, suggesting that Dclk1+ cells may provide a useful surrogate for evaluating  
310 the survival of ISCs following radiation injury. A recent report by Hua et al. has shown that  
311 following 12 Gy TBI, the Lgr5 labeled crypt based columnar stem cells undergo apoptosis  
312 starting at 6 h and peaking at 24 h, followed by mitotic death at 24-48 h post TBI (12). Their  
313 results suggest that examining at 24 h time point may overestimate the number of surviving  
314 stem cells, and the surviving stem cells at 48 h may better predict crypt regeneration at 3.5  
315 d post TBI (12).

316

317 Notch signaling has been implicated in stem cell maintenance in many systems  
318 through its downstream target Hes1 (5). Notch signaling drives progenitor cells towards an  
319 enterocyte lineage, while inhibition of Notch signaling drives progenitor cells towards a  
320 secretory lineage resulting in an abundance of Goblet cells (17). Despite this seemingly  
321 protective phenotype, Notch inhibitors were not protective against colitis induced by the  
322 chemical irritant DSS. Moreover, Notch inhibition appears to exacerbate colitis in other  
323 models of inflammatory injury (20). In addition, gut toxicity has been a major limiting factor  
324 in many clinical trials of Notch inhibitors for a variety of liquid tumors. This toxicity can be  
325 attenuated by limiting the dosing schedule to every 4 days allowing for recovery of the  
326 intestinal epithelium which turns over every 3-4 days. This may represent a plausible  
327 explanation for the improved tolerability of this regimen. These data led us to investigate

328 whether stem cells were actually deleted or at least functionally inhibited by Notch  
329 inhibition. Our results demonstrate that systemic Notch inhibition beginning 24 h prior to IR  
330 results in a 50% reduction in crypt survival after IR compared to vehicle treated controls,  
331 suggesting that inhibition of Notch can functionally reduce ISC's activity. This result seems  
332 to confirm the well-known role of the Notch pathway in stem cell biology, and these studies  
333 demonstrate a direct effect of Notch inhibition on intestinal stem cells in vivo.

334 To further analyze this result mechanistically, we sought to determine the effect of  
335 Notch inhibition on the expression of the putative ISC marker Dclk1 in response to radiation  
336 injury. In response to DAPT treatment alone without radiation injury, we found an  
337 approximately 20% decrease in Dclk1 mRNA levels, but no change in the number of  
338 Dclk1+ cells per cross section. Since the Dclk1+ cells were detected by immunostaining, it  
339 may not be sensitive enough to detect small changes in Dclk1 protein levels. We have  
340 reported that treating HCT116 colon cancer xenografts with DAPT results in both Dclk1  
341 mRNA and protein downregulation in the tumor, suggesting a Notch regulatory mechanism  
342 (33). We evaluated the effects of radiation injury on Dclk1 expression 24 h post IR, the  
343 postulated time point at which p53 independent stem cell apoptosis occurs following lethal  
344 dose IR (14, 16). We chose Dclk1 for several reasons: 1) its limited expression pattern  
345 within the crypt allowed for quantitative assessment; 2) its distinct subcellular expression  
346 pattern in conjunction with labeling with nuclear markers (such as p- $\beta$ -cat-Ser552) within a  
347 particular crypt could be used to determine the identity of DNA damaged cells; and 3) other  
348 putative stem cell markers are expressed in crypt based columnar and progenitor  
349 populations making it impossible to quantitatively assess the effects of Notch inhibition on  
350 crypt dynamics in two dimensional histologic sections (24). Although skepticism still exists

351 regarding the identity of Dclk1 expressing cells (8), there is increasing data in other models  
352 suggesting that Dclk1 plays a functional role in many cancers and is unlikely to be a marker  
353 of wholly differentiated cells. Studies are currently underway to determine the function of  
354 Dclk1 in the gut in normal homeostasis and in cancer. The possibility that Dclk1 and other  
355 markers that are observed at the +4 position (i.e. Msi1, Bmi1, Lrig1, and mTert) (18, 23,  
356 29, 31, 34, 39) may serve to mark “rescue stem cells” in response to severe  
357 genotoxic/cytotoxic injury must also be considered.

358 The studies presented here attempt to assess the role of Notch signaling on  
359 epithelial crypt stem cell fate in response to genotoxic/cytotoxic injury using Dclk1 as an *in*  
360 *situ* marker of reserve or rescue stem cells. Notch signaling may play a key role as a  
361 regulatory mechanism for protection of the stem cell under severe DNA damage. Recent  
362 studies using Notch deficient mice have demonstrated that Notch deletion results in a  
363 reduction in Wnt target genes including the novel stem cell marker Lgr5 (21). These  
364 findings suggest in a correlative manner that Notch may be upstream of Wnt with respect to  
365 stem cell dynamics and that Notch inhibition may indeed result in reduced Wnt signaling.  
366 This combined reduction in stem cell pathway signaling may be a welcome approach in  
367 attenuating the stem cell phenotype in cancer by reducing the cell of origin as well as the  
368 proliferative potential of the stem cell offspring. This hypothesis would certainly be in play if  
369 a hierarchical or interconversion model of the stem cell niche were the reality. Because the  
370 identity and validation of novel stem cell markers continues to be debated, functional  
371 assays of stem cell survival such as clonogenic microcolony assays remain necessary.  
372 Evaluation of Dclk1 expression in radiation and related injury models may serve as an  
373 effective model to test the effects of therapeutic agents on gut stem cells directly. This use



374 of Dclk1 is currently feasible as commercial antibodies that are easy to use and yield  
375 reproducible results in many tissues are available. Furthermore, the expression in a  
376 minority of cells allow for quantitative assessment of the response to genotoxic/cytotoxic  
377 injury particularly 24 h after radiation injury. We are aware of reports that Dclk1 represents  
378 a fully differentiated Tuft cell or enteroendocrine cell based on immunohistochemistry (8).  
379 We contend the functional properties of Dclk1 and previous reported sorting studies identify  
380 a subset of Dclk1 cells that are not fully differentiated. In fact, a recent study by Bjerknes *et*  
381 *al.* confirmed the presence of an early Tuft cell in the crypt with a different marker  
382 expression profile (1). Finally, there is a possibility that a subset of tuft cells has stem cell  
383 like properties. In fact, several recent reports suggest that other cell types can revert to  
384 stem cells upon crypt damage (2, 35, 36). Using a transgenic mouse model (Cyp1A1-H2B-  
385 YFP), Buczacki *et al* reported that label-retaining cells (Histone 2B positive) at the crypt  
386 base of the small intestine have a combined secretory and stem-cell signature, and  
387 demonstrate clonogenicity after injury (2). Additionally, Van Es *et al.* showed that Dll1+  
388 secretory progenitor cells can revert to stem cells during intestinal crypt regeneration  
389 following injury (35). Using the Sox9-EGFP transgenic mouse model, Van Landeghem *et*  
390 *al.* found that Sox9-EGFP high cells have both an enteroendocrine and a +4 ISC signature,  
391 and express Dclk1 protein. Moreover, isolated Sox9-EGFP high cells form organoids *in*  
392 *vitro* after radiation injury, suggesting that Sox9-EGFP high cells contain radiation-activated  
393 cells with ISC characteristics that likely participate in crypt regeneration post injury (36). A  
394 recent report by Nakanishi *et al.* shown that there was no detectable BrdU incorporation in  
395 Dclk1+ cells in the normal intestine, and extremely small number of blue stripes comprised  
396 LacZ-labeled Dclk1+ cell lineages 14 days after 8 Gy IR in the Dclk1-Cre-ERT2 lineage

397 tracing mouse (19). It is hypothesized that the +4 position quiescent stem cell is a potential  
398 rescue stem cell, and may play a minor role in normal intestinal homeostasis where Lgr5+  
399 rapidly cycling stem/progenitor cells may have a predominant role. In this report, they used  
400 8 Gy IR to activate lineage tracing. However, it may be necessary to use a > 8 Gy high  
401 dose IR to functionally achieve lineage tracing from a “rescue stem cell”.

402           The results reported here lend additional support to the hypothesis that the Notch  
403 signaling pathway is a valid target for anti-stem cell based therapies. Furthermore, these  
404 studies provide a reasonable explanation for the side effect profile observed with GSIs and  
405 establish Dclk1 expression as an effective marker for testing the effects of therapeutic  
406 agents in radiation and related injury models. Additional approaches to the inhibition of the  
407 Notch signaling pathway may be beneficial for anti-cancer drug development.

408

409 **Grants:** This research was performed as a project of the Intestinal Stem Cell Consortium;  
410 a collaborative research project funded by the National Institute of Diabetes and Digestive  
411 and Kidney Diseases and the National Institute of Allergy and Infectious Diseases (NIH  
412 U01 DK-085508 to CWH) and also funded by a Veterans Affairs Merit Award to CWH.

413

414 **Disclosures:** C.W. Houchen is a founder of COARE Biotechnology, Inc. The other authors  
415 have declared that no conflict of interest exists.

416

417

418 **References:**

419

- 420 1. **Bjerknes M, Khandanpour C, Moroy T, Fujiyama T, Hoshino M, Klisch TJ, Ding**  
421 **Q, Gan L, Wang J, Martin MG, and Cheng H.** Origin of the brush cell lineage in the  
422 mouse intestinal epithelium. *Developmental biology* 362: 194-218, 2012.
- 423 2. **Buczacki SJ, Zecchini HI, Nicholson AM, Russell R, Vermeulen L, Kemp R, and**  
424 **Winton DJ.** Intestinal label-retaining cells are secretory precursors expressing Lgr5. *Nature*  
425 495: 65-69, 2013.
- 426 3. **Cheng H, and Leblond CP.** Origin, differentiation and renewal of the four main  
427 epithelial cell types in the mouse small intestine. V. Unitarian Theory of the origin of the four  
428 epithelial cell types. *The American journal of anatomy* 141: 537-561, 1974.
- 429 4. **Cohn SM, Simon TC, Roth KA, Birkenmeier EH, and Gordon JI.** Use of  
430 transgenic mice to map cis-acting elements in the intestinal fatty acid binding protein gene  
431 (Fabpi) that control its cell lineage-specific and regional patterns of expression along the  
432 duodenal-colonic and crypt-villus axes of the gut epithelium. *J Cell Biol* 119: 27-44, 1992.
- 433 5. **Fre S, Hannezo E, Sale S, Huyghe M, Lafkas D, Kissel H, Louvi A, Greve J,**  
434 **Louvard D, and Artavanis-Tsakonas S.** Notch lineages and activity in intestinal stem cells  
435 determined by a new set of knock-in mice. *PLoS One* 6: e25785, 2011.
- 436 6. **Fre S, Huyghe M, Mourikis P, Robine S, Louvard D, and Artavanis-Tsakonas S.**  
437 Notch signals control the fate of immature progenitor cells in the intestine. *Nature* 435: 964-  
438 968, 2005.
- 439 7. **George RJ, Sturmoski MA, May R, Sureban SM, Dieckgraefe BK, Anant S, and**  
440 **Houchen CW.** Loss of p21Waf1/Cip1/Sdi1 enhances intestinal stem cell survival following  
441 radiation injury. *American journal of physiology Gastrointestinal and liver physiology* 296:  
442 G245-254, 2009.
- 443 8. **Gerbe F, van Es JH, Makrini L, Brulin B, Mellitzer G, Robine S, Romagnolo B,**  
444 **Shroyer NF, Bourgaux JF, Pignodel C, Clevers H, and Jay P.** Distinct ATOH1 and  
445 Neurog3 requirements define tuft cells as a new secretory cell type in the intestinal  
446 epithelium. *The Journal of cell biology* 192: 767-780, 2011.
- 447 9. **Gordon JI, and Hermiston ML.** Differentiation and self-renewal in the mouse  
448 gastrointestinal epithelium. *Curr Opin Cell Biol* 6: 795-803, 1994.
- 449 10. **He XC, Yin T, Grindley JC, Tian Q, Sato T, Tao WA, Dirisina R, Porter-**  
450 **Westpfahl KS, Hembree M, Johnson T, Wiedemann LM, Barrett TA, Hood L, Wu H,**  
451 **and Li L.** PTEN-deficient intestinal stem cells initiate intestinal polyposis. *Nat Genet* 39:  
452 189-198, 2007.
- 453 11. **Houchen CW, George RJ, Sturmoski MA, and Cohn SM.** FGF-2 enhances  
454 intestinal stem cell survival and its expression is induced after radiation injury. *Am J Physiol*  
455 276: G249-258, 1999.
- 456 12. **Hua G, Thin TH, Feldman R, Haimovitz-Friedman A, Clevers H, Fuks Z, and**  
457 **Kolesnick R.** Crypt base columnar stem cells in small intestines of mice are radioresistant.  
458 *Gastroenterology* 143: 1266-1276, 2012.
- 459 13. **Koch U, Lehal R, and Radtke F.** Stem cells living with a Notch. *Development* 140:  
460 689-704, 2013.
- 461 14. **May R, Riehl TE, Hunt C, Sureban SM, Anant S, and Houchen CW.** Identification  
462 of a novel putative gastrointestinal stem cell and adenoma stem cell marker, doublecortin

463 and CaM kinase-like-1, following radiation injury and in adenomatous polyposis coli/multiple  
464 intestinal neoplasia mice. *Stem Cells* 26: 630-637, 2008.

465 15. **May R, Sureban SM, Hoang N, Riehl TE, Lightfoot SA, Ramanujam R, Wyche**  
466 **JH, Anant S, and Houchen CW.** Doublecortin and CaM kinase-like-1 and leucine-rich-  
467 repeat-containing G-protein-coupled receptor mark quiescent and cycling intestinal stem  
468 cells, respectively. *Stem Cells* 27: 2571-2579, 2009.

469 16. **Merritt AJ, Allen TD, Potten CS, and Hickman JA.** Apoptosis in small intestinal  
470 epithelial from p53-null mice: evidence for a delayed, p53-independent G2/M-associated  
471 cell death after gamma-irradiation. *Oncogene* 14: 2759-2766, 1997.

472 17. **Milano J, McKay J, Dagenais C, Foster-Brown L, Pognan F, Gadiant R, Jacobs**  
473 **RT, Zacco A, Greenberg B, and Ciaccio PJ.** Modulation of notch processing by gamma-  
474 secretase inhibitors causes intestinal goblet cell metaplasia and induction of genes known  
475 to specify gut secretory lineage differentiation. *Toxicol Sci* 82: 341-358, 2004.

476 18. **Montgomery RK, Carlone DL, Richmond CA, Farilla L, Kranendonk ME,**  
477 **Henderson DE, Baffour-Awuah NY, Ambruzs DM, Fogli LK, Algra S, and Breault DT.**  
478 Mouse telomerase reverse transcriptase (mTert) expression marks slowly cycling intestinal  
479 stem cells. *Proceedings of the National Academy of Sciences of the United States of*  
480 *America* 108: 179-184, 2011.

481 19. **Nakanishi Y, Seno H, Fukuoka A, Ueo T, Yamaga Y, Maruno T, Nakanishi N,**  
482 **Kanda K, Komekado H, Kawada M, Isomura A, Kawada K, Sakai Y, Yanagita M,**  
483 **Kageyama R, Kawaguchi Y, Taketo MM, Yonehara S, and Chiba T.** Dclk1 distinguishes  
484 between tumor and normal stem cells in the intestine. *Nature genetics* 2012.

485 20. **Okamoto R, Tsuchiya K, Nemoto Y, Akiyama J, Nakamura T, Kanai T, and**  
486 **Watanabe M.** Requirement of Notch activation during regeneration of the intestinal  
487 epithelia. *Am J Physiol Gastrointest Liver Physiol* 296: G23-35, 2009.

488 21. **Pellegrinet L, Rodilla V, Liu Z, Chen S, Koch U, Espinosa L, Kaestner KH,**  
489 **Kopan R, Lewis J, and Radtke F.** Dll1- and dll4-mediated notch signaling are required for  
490 homeostasis of intestinal stem cells. *Gastroenterology* 140: 1230-1240 e1231-1237, 2011.

491 22. **Potten CS.** A comprehensive study of the radiobiological response of the murine  
492 (BDF1) small intestine. *International journal of radiation biology* 58: 925-973, 1990.

493 23. **Potten CS, Booth C, and Hargreaves D.** The small intestine as a model for  
494 evaluating adult tissue stem cell drug targets. *Cell proliferation* 36: 115-129, 2003.

495 24. **Potten CS, Gandara R, Mahida YR, Loeffler M, and Wright NA.** The stem cells of  
496 small intestinal crypts: where are they? *Cell Prolif* 42: 731-750, 2009.

497 25. **Potten CS, and Grant HK.** The relationship between ionizing radiation-induced  
498 apoptosis and stem cells in the small and large intestine. *British journal of cancer* 78: 993-  
499 1003, 1998.

500 26. **Potten CS, and Loeffler M.** A comprehensive model of the crypts of the small  
501 intestine of the mouse provides insight into the mechanisms of cell migration and the  
502 proliferation hierarchy. *J Theor Biol* 127: 381-391, 1987.

503 27. **Potten CS, and Loeffler M.** Stem cells: attributes, cycles, spirals, pitfalls and  
504 uncertainties. Lessons for and from the crypt. *Development* 110: 1001-1020, 1990.

505 28. **Potten CS, Merritt A, Hickman J, Hall P, and Faranda A.** Characterization of  
506 radiation-induced apoptosis in the small intestine and its biological implications.  
507 *International journal of radiation biology* 65: 71-78, 1994.

- 508 29. **Potten CS, Owen G, and Booth D.** Intestinal stem cells protect their genome by  
509 selective segregation of template DNA strands. *Journal of cell science* 115: 2381-2388,  
510 2002.
- 511 30. **Riehl TE, George RJ, Sturmoski MA, May R, Dieckgraefe B, Anant S, and**  
512 **Houchen CW.** Azoxymethane protects intestinal stem cells and reduces crypt epithelial  
513 mitosis through a COX-1-dependent mechanism. *Am J Physiol Gastrointest Liver Physiol*  
514 291: G1062-1070, 2006.
- 515 31. **Sangiorgi E, and Capecchi MR.** Bmi1 is expressed in vivo in intestinal stem cells.  
516 *Nature genetics* 40: 915-920, 2008.
- 517 32. **Schmidt GH, Wilkinson MM, and Ponder BA.** Cell migration pathway in the  
518 intestinal epithelium: an in situ marker system using mouse aggregation chimeras. *Cell* 40:  
519 425-429, 1985.
- 520 33. **Sureban SM, May R, Mondalek FG, Qu D, Ponnurangam S, Pantazis P, Anant S,**  
521 **Ramanujam RP, and Houchen CW.** Nanoparticle-based delivery of siDCAMKL-1  
522 increases microRNA-144 and inhibits colorectal cancer tumor growth via a Notch-1  
523 dependent mechanism. *Journal of nanobiotechnology* 9: 40, 2011.
- 524 34. **Tian H, Biehs B, Warming S, Leong KG, Rangell L, Klein OD, and de Sauvage**  
525 **FJ.** A reserve stem cell population in small intestine renders Lgr5-positive cells  
526 dispensable. *Nature* 478: 255-259, 2011.
- 527 35. **van Es JH, Sato T, van de Wetering M, Lyubimova A, Nee AN, Gregorieff A,**  
528 **Sasaki N, Zeinstra L, van den Born M, Korving J, Martens AC, Barker N, van**  
529 **Oudenaarden A, and Clevers H.** Dll1+ secretory progenitor cells revert to stem cells upon  
530 crypt damage. *Nature cell biology* 14: 1099-1104, 2012.
- 531 36. **Van Landeghem L, Santoro MA, Krebs AE, Mah AT, Dehmer JJ, Gracz AD,**  
532 **Scull BP, McNaughton K, Magness ST, and Lund PK.** Activation of two distinct Sox9-  
533 EGFP-expressing intestinal stem cell populations during crypt regeneration after irradiation.  
534 *American journal of physiology Gastrointestinal and liver physiology* 302: G1111-1132,  
535 2012.
- 536 37. **Winton DJ, and Ponder BA.** Stem-cell organization in mouse small intestine. *Proc*  
537 *Biol Sci* 241: 13-18, 1990.
- 538 38. **Withers HR, and Elkind MM.** Microcolony survival assay for cells of mouse  
539 intestinal mucosa exposed to radiation. *International journal of radiation biology and related*  
540 *studies in physics, chemistry, and medicine* 17: 261-267, 1970.
- 541 39. **Wong VW, Stange DE, Page ME, Buczacki S, Wabik A, Itami S, van de Wetering**  
542 **M, Poulson R, Wright NA, Trotter MW, Watt FM, Winton DJ, Clevers H, and Jensen**  
543 **KB.** Lrig1 controls intestinal stem-cell homeostasis by negative regulation of ErbB  
544 signalling. *Nat Cell Biol* 2012.
- 545
- 546

547 **Figure Legends**

548

549 **Figure 1. The intestinal crypts response to radiation injury.** Wild type C57Bl/6 mice  
550 were subjected to 12 Gy IR. The small intestinal crypts isolated 6, 24, 84, and 168 h post IR  
551 were stained with H&E and presented. The magnification is 400x.

552

553 **Figure 2. Identification of Dclk1 positive apoptotic cells in small intestinal crypts**  
554 **after TBI.** The small intestine isolated 6 and 24 h post TBI were fixed with formalin and  
555 embedded in paraffin. Paraffin-embedded sections were immunostained with anti-Dclk1  
556 antibody (red in the left panel) and ApopTag Peroxidase for apoptotic cells (green in the  
557 middle panel). Co-localization of Dclk1 (red) in apoptotic cells (green) is indicated by arrows  
558 in the overlay pictures (right panel). Upper panels are 6 h post TBI and lower panels are 24  
559 h post TBI. The magnification is 200x, and the magnification for the inset is ~600x.

560

561 **Figure 3. Identification of Dclk1 positive mitotic cells in small intestinal crypts after**  
562 **TBI.** The small intestine isolated 24 h post TBI were fixed with formalin and embedded in  
563 paraffin. Paraffin-embedded sections were immunostained with anti-Dclk1 antibody (purple,  
564 purple arrow) and anti-phospho  $\beta$ -catenin Ser552 antibody (brown, black arrow). Co-  
565 localization of Dclk1 with phospho  $\beta$ -catenin was indicated by arrowhead. The  
566 magnification is 400x.

567

568 **Figure 4. Identification of Dclk1 positive proliferative cells in small intestinal crypts**  
569 **after TBI.** The small intestine isolated 24 h post TBI were fixed with formalin and  
570 embedded in paraffin. Paraffin-embedded sections were immunostained with anti-Dclk1

571 antibody (purple) and anti-Ki67 antibody (brown) (**A**). Co-localization of Dclk1 with Ki67 was  
572 indicated by arrow. The magnification for the inset is ~600x (**B**).

573

574 **Figure 5. Inhibition of Notch1 signaling pathway reduced surviving Dclk1 positive**  
575 **cells after radiation injury.** C57Bl/6 mice in control group (**A**) or DAPT treated group (**B**)  
576 are subjected to TBI. 24 h post IR, the small intestines were isolated, fixed, processed, and  
577 stained with anti-Dclk1 antibody. Dclk1 positive cells in one cross section were indicated by  
578 arrows in panels A and B. The magnification is 40x for the cross section pictures, and  
579 ~600x for the inset. The average number of Dclk1 positive cells per cross section was  
580 counted for total of 80 cross sections and presented in panel **C**. Values in the bar graph are  
581 given as average  $\pm$  SEM and \* denote statistically significant difference ( $*p<0.01$ )  
582 compared to control.

583

584 **Figure 6. Inhibition of Notch1 signaling pathway reduced the number of surviving**  
585 **crypts after radiation injury.** C57Bl/6 mice in control group (**A**) or DAPT treated group (**B**)  
586 were subjected to TBI. These mice were injected with BrdU solution 82 h post IR, and killed  
587 84 h post IR. The small intestines were isolated, fixed, and processed. BrdU positive cells  
588 are the indication for surviving crypts in panels **A** and **B**. The magnification is 40x for the  
589 cross section pictures, and ~600x for the inset. The average number of surviving crypts per  
590 cross section was counted for total of 80 cross sections and presented in panel **C**. Values  
591 in the bar graph are given as average  $\pm$  SEM and \* denote statistically significant  
592 difference ( $*p<0.01$ ) compared to control.

593

594 **Figure 7. Inhibition of Notch1 signaling pathway decreased Dclk1 mRNA expression**  
595 **after TBI.** Total RNAs were isolated from the small intestine after each treatment. mRNA  
596 expression levels were measured by quantitative real-time RT-PCR, and normalized  
597 against  $\beta$ -actin level. **A.** Dclk1 mRNA after DAPT and radiation injury. **B.** Notch1 mRNA  
598 after DAPT and radiation injury. **C.** Hes1 mRNA after DAPT and radiation injury. Values in  
599 the bar graphs are given as average  $\pm$  SEM and \* denote statistically significant difference  
600 (\* $p$ <0.05) compared to control.

601

602

603

604

605

606

607

608

609

610

611

612

613



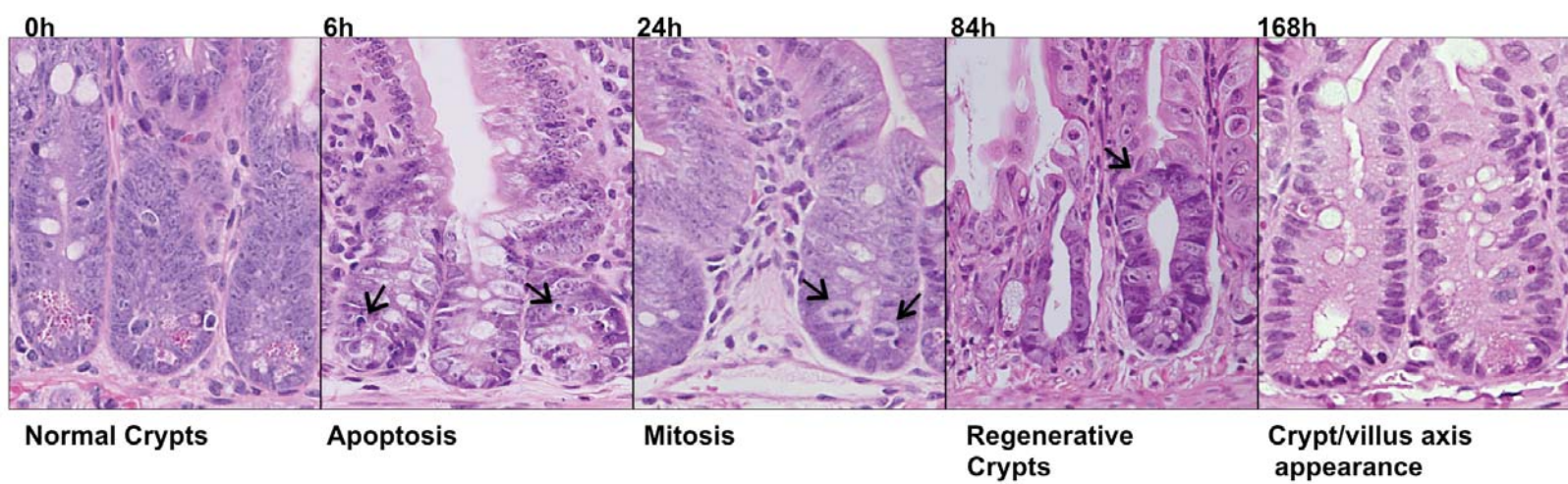


Figure 1.

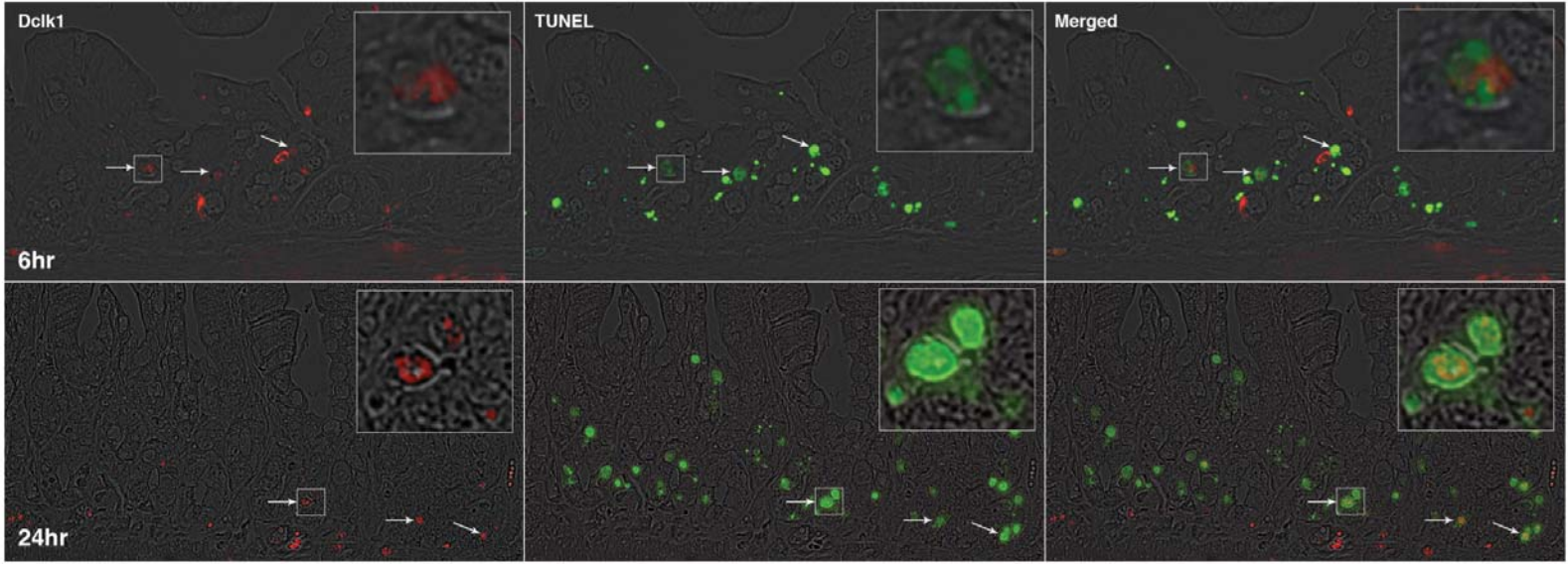


Figure 2.

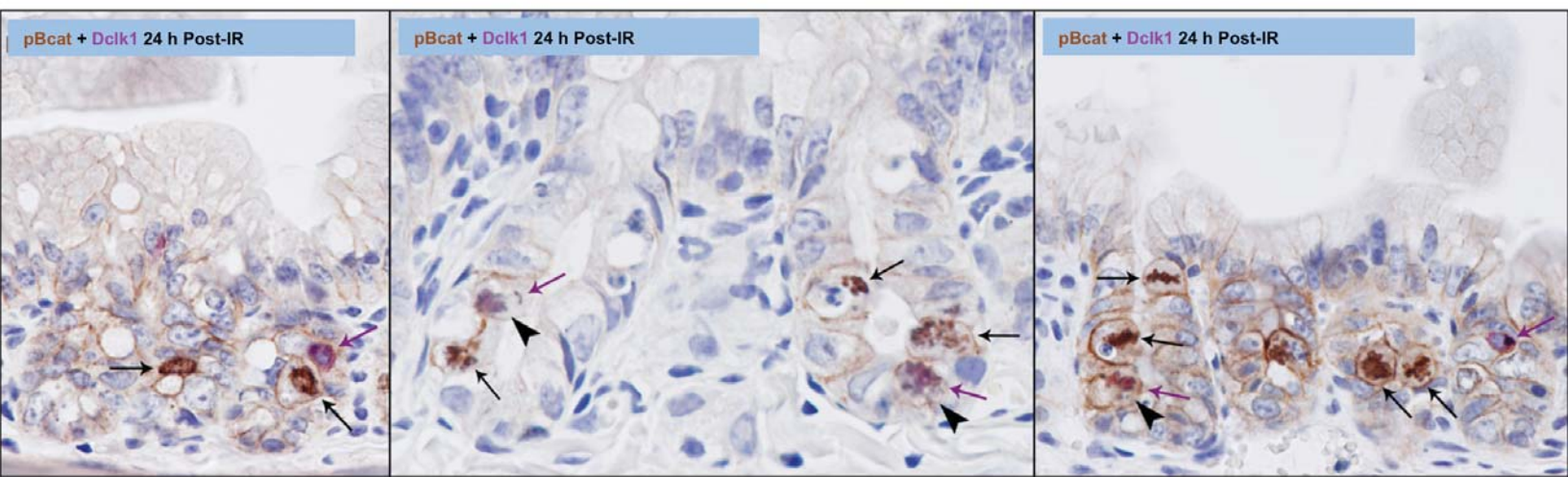
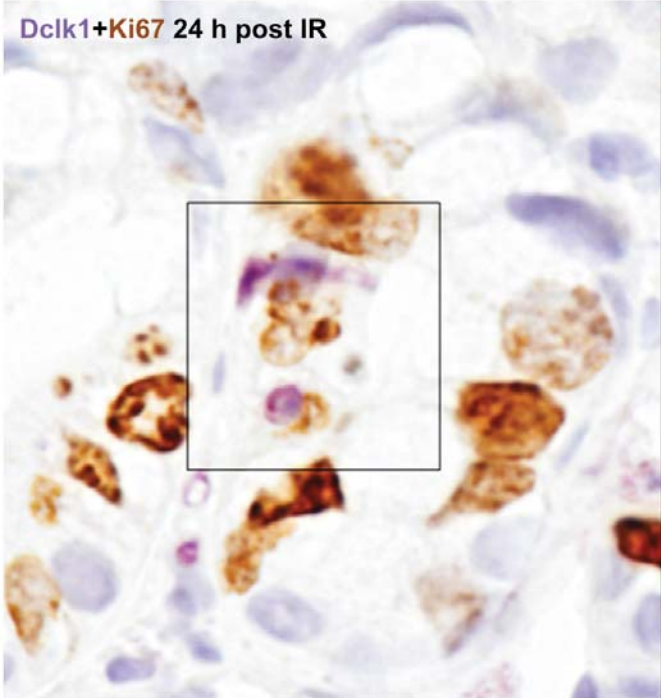


Figure 3.

**A.**

Dclk1+Ki67 24 h post IR



**B.**

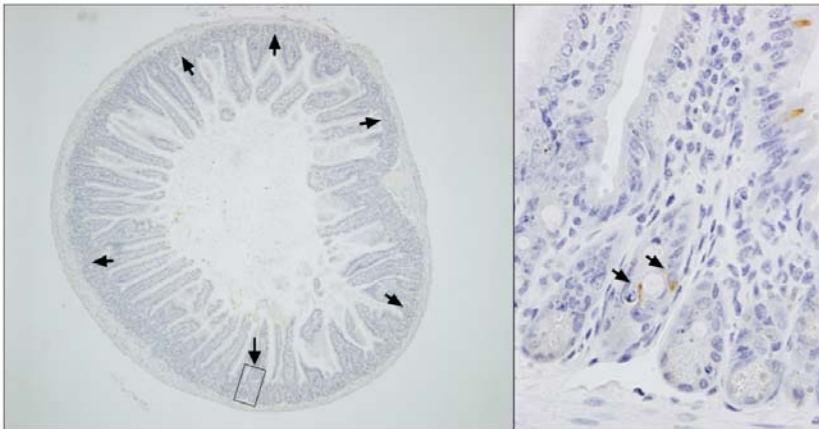


**Figure 4**

**A. Control**



**B. +DAPT**



**C.**

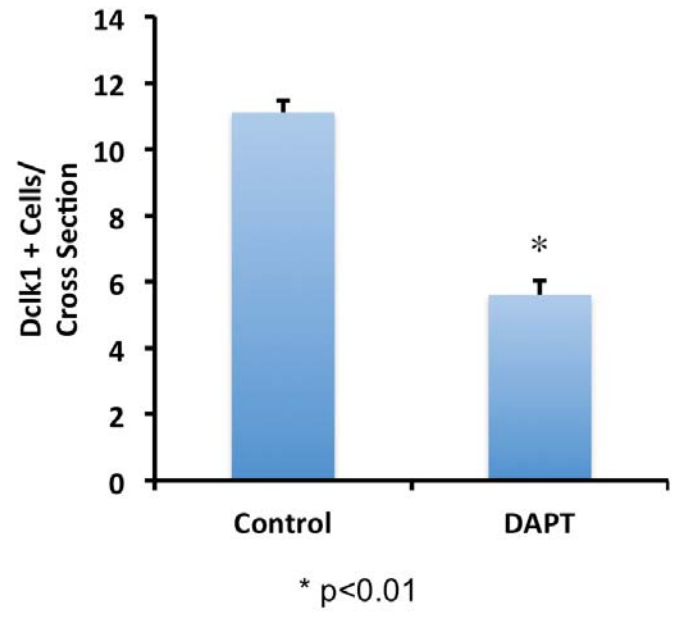
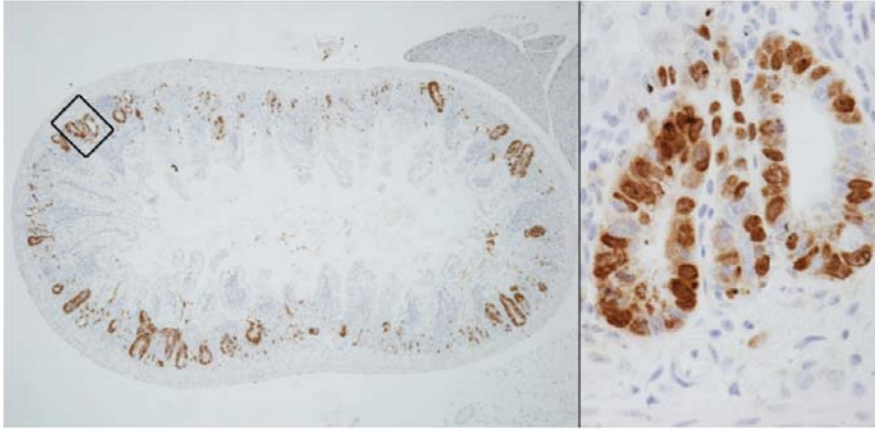
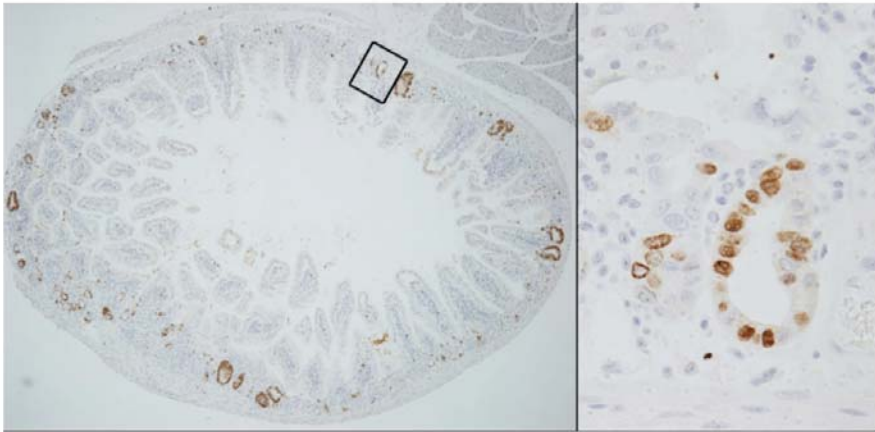


**Figure 5.**

**A. Control**



**B. +DAPT**



**C.**

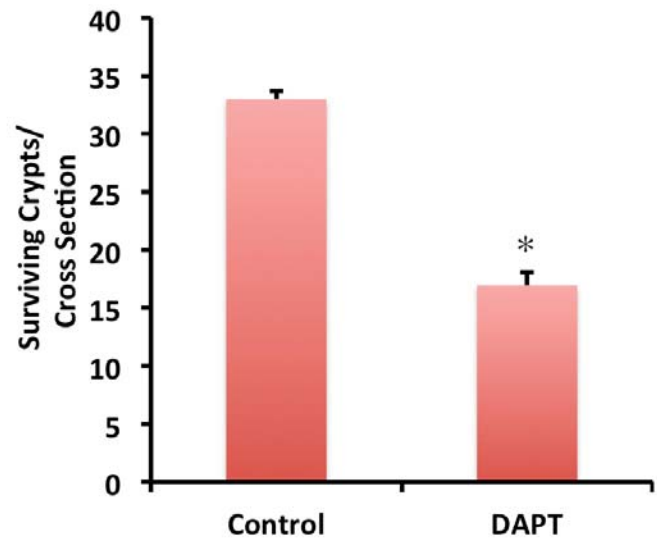
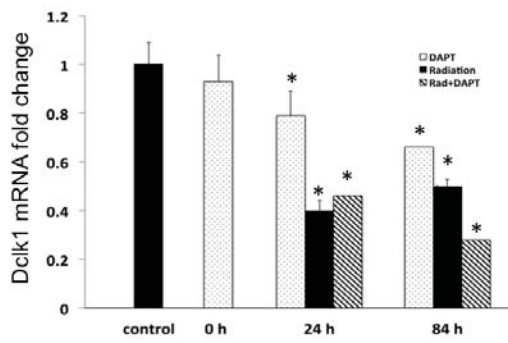
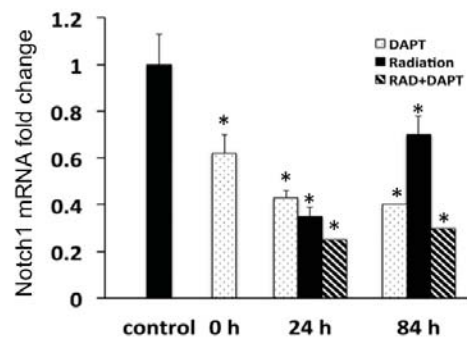


**Figure 6.**

### A. Dclk1



### B. Notch1



### C. Hes1

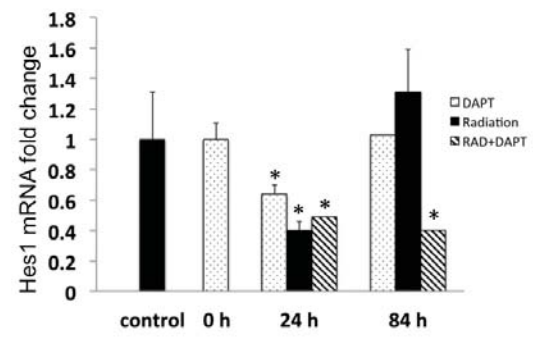


Figure 7.